Carbohydrate Polymers 77 (2009) 599–606

Contents lists available at ScienceDirect

Carbohydrate Polymers

journal homepage: www.elsevier.com/locate/carbpol

Evaluation of Alginate/Chitosan nanoparticles as antisense delivery vector: Formulation, optimization and in vitro characterization

Tarane Gazori [a], Mohammad Reza Khoshayand [b], Ebrahim Azizi [c], Parisa Yazdizade [d], Alireza Nomani [a,e], Ismaeil Haririan [a,f,*]

[a] Department of Pharmaceutics, Faculty of Pharmacy, Tehran University of Medical Sciences, Enghelab Street, Tehran 14155-6451, Iran
[b] Department of Drug and Food Control, Faculty of Pharmacy and Pharmaceutical Research Center, Tehran University of Medical Sciences, Tehran, Iran
[c] Cellular and Molecular Laboratory, Department of Toxicology, Faculty of Pharmacy, Tehran University of Medical Sciences, Tehran, Iran
[d] Azad University, Pharmaceutical Sciences Branch, Tehran, Iran
[e] School of Pharmacy, Zanjan University of Medical Sciences, Zanjan, Iran
[f] Biomaterial Research Center (BRC), Tehran, Iran

ARTICLE INFO

Article history:
Received 22 December 2008
Received in revised form 26 January 2009
Accepted 2 February 2009
Available online 24 February 2009

Keywords:
Chitosan
Alginate
Nanoparticles
Pregel preparing method
EGFR antisense
Optimization
Experimental design

ABSTRACT

Nanoparticles comprising Alginate/Chitosan polymers were prepared by pregel preparation method through drop wise addition of various concentrations of $CaCl_2$ to a defined concentration of Sodium Alginate. Then, Chitosan/Antisense solution with a certain N/P ratio was added to the pregel to make the nanoparticles. The effect of such parameters as polymer ratio, $CaCl_2$/Alginate ratio and N/P ratio on the particle size distribution and loading efficacy was studied. The optimum conditions were 1:1 (w/w) Alginate to Chitosan ratio, 0.2% $CaCl_2$/Alginate ratio and N/P ratio of 5 at pH 5.3. The resulting nanoparticles had a loading efficacy of 95.6% and average size of 194 nm as confirmed by PCS method and SEM images showed spherical and smooth particles. The zeta potential of optimized nanoparticles prepared by this method was about +30 mV which could result in good stability of nanoparticles during manipulation and storage.

1. Introduction

The use of natural biopolymers specifically polysaccharides in drug delivery has attracted particular interest due to their desirable biocompatible, biodegradable, hydrophilic and protective properties (Barichello, Morishita, Takayama, & Nagai, 1999). The interaction between biodegradable cationic and anionic biopolymers leads to the formation of polyionic hydrogels, which have demonstrated favorable characteristics for drug entrapment and delivery (Chellat et al., 2000).

Chitosan and Alginate are two biopolymers that have received much attention and been extensively studied for such a use. Entrapment in biopolymers of therapeutic agents including: peptides, proteins and polynucleotides have been shown to maintain their structure and activity and protect them from enzymatic degradation (Madan et al., 1997). Moreover, many of these polymers, particularly hydrogels, are naturally hydrophilic, which is advantageous since this property is thought to contribute to longer *in vivo* circulation times and allows encapsulation of water-soluble biomolecules (Douglas & Tabrizian, 2005).

Chitosan is a natural cationic polysaccharide obtained by the N-deacetylation of chitin, a product found in the shells of crustaceans. It is widely used as a carrier in gene delivery, oral protein delivery and controlled release systems (Borchard, 2001; Mansouri et al., 2004).

Alginate is an anionic polysaccharide consisting of linear copolymers of α-L-guluronate and β-D-mannuronate residues. Alginates which are a group of hemocompatible polymers have not been found to accumulate in any major organs and have shown evidence of *in vivo* degradation (Mi, Sung, & Shyu, 2002). In the presence of Calcium ions, ionic interactions between the divalent Calcium ions and the guluronic acid residues cause Alginates to form gels. The properties of Calcium–Alginate gel beads make them one of the most widely used carriers for controlled release systems (Fundueanu, Nastruzzi, Carpov, Desbrieres, & Rinaudo, 1999). Coating of these beads with other polymers including Chitosan has been shown to improve their stability during (shelf-life) storage and their half life in biological fluids.

* Corresponding author. Address: Department of Pharmaceutics, Faculty of Pharmacy, Tehran University of Medical Sciences, Enghelab Street, Tehran 14155-6451, Iran. Tel./fax: +98 21 66482607.
E-mail address: haririan@tums.ac.ir (I. Haririan).

0144-8617/$ - see front matter Crown Copyright © 2009 Published by Elsevier Ltd. All rights reserved.
doi:10.1016/j.carbpol.2009.02.019

Alginate–Chitosan polyionic complexes form through ionic gelation *via* interactions between the carboxyl groups of Alginate and the amine groups of Chitosan. The complex protects the encapsulant, has biocompatible and biodegradable characteristics, and limits the release of encapsulated materials more effectively than either Alginate or Chitosan alone (Yan, Khor, & Lim, 2001). A further advantage of this delivery system is its non-toxicity, which permits its administration to be repeated as a therapeutic agent. Alginate–Chitosan (Alg/Chi) microspheres or beads have been widely studied for the encapsulation of drugs, oligonucleotides, proteins and cells, with promising results (De and Robinson, 2003). Despite the attractive properties of this system, its development and application in the submicron scale has rarely been studied (Douglas & Tabrizian, 2005).

Because of the desirable characteristics and demonstrated success of the Alg/Chi system, the development and use of this system on the submicron scale and its potential use as a gene carrier needs to be evaluated. Therefore, the purpose of this study was to optimize a method for the preparation of Alg/Chi nanoparticles by the use of Box–Behnken methodology to design the most appropriate preparation method.

Antisense oligonucleotides (ODNs) targeted to the epidermal growth factor receptor (EGFR) was chosen as a single strand nucleic acid model which were entrapped in these optimized nanoparticles; a receptor tyrosine kinase proto-oncogene that plays a central role in the initiation and development of several human malignancies, notably breast, brain, and lung tumors (Arteaga, 2002). For this purpose, Alg/Chi nanoparticles were prepared using Sodium Alginate and Calcium Chloride and adding Chitosan/Antisense solution to the pregel for preparing nanoparticles. The influence of various experimental parameters on the formation of nanoparticles, including different ratios of the biopolymers, Calcium Chloride/Alginate ($CaCl_2$/Alg %) and N/P ratios (the stoichiometric ratio of antisense phosphate groups; P to Chitosan amine groups; N) have been investigated. N/P ratio can affect zeta potential, particle size, loading efficacy and also transfection efficacy of antisense oligonucleotides (Kim & Kim, 2007), the subject is in progress in my study and will be reported in our future paper. The nanoparticulate formulation of EGFR antisense was optimized using design of experiments by employing response surface methodology.

Response surface methodology determines the optimum level of each factor by building a mathematical model. Optimization of particle size and loading efficacy as the responses were carried out by Box–Behnken response surface methodology.

2. Materials and methods

2.1. Materials

Sodium Alginate (BDH Co., UK), low molecular weight Chitosan (Sigma–Aldrich Co., Germany), and Calcium Chloride (Merck KGaA Co., Germany), EGFR Phosphorothioated 21 mer antisense 5′ (TTT CTT TTC CTC CAG AGC CCG) 3′ (TIB MOL BIOL® GmbH, Germany) were purchased and used as received.

2.2. Nanoparticle preparation

2.2.1. Stock solutions

Stock solution of Sodium Alginate and Calcium Chloride was prepared by dissolving 500 mg of each material in 50 ml of deionized water, respectively. Five hundred milligrams of Chitosan was then dissolved in 50 ml of 1% (V/V) acetic acid. Freeze dried powder of EGFR antisense was dissolved with DEPC (diethylpyrocarbonate) treated water to make a 100 μM stock solution. All the stock solutions were filtered (0.22 μm syringe filter) prior to use.

2.2.2. Pregel preparation method

With respect to Alg/Chi ratio a certain amount of Sodium Alginate stock solution was diluted with 10 ml of filtered deionized water. Then 1 ml of Calcium Chloride solution adjusted to Ca/Alg % ratio was added drop wise to above solution while stirring. The prepared Ca/Alg pregel was stirred for a further 10 min. Chitosan solutions were prepared according to N/P ratios and different Alg/Chi ratios, as listed in Table 1. Then 5 μl of 100 μM of EGFR antisense solution was added to it. It was stirred for 10 min to be complexed, then added drop wise to Calcium Alginate pregel, while stirring. In cases where the pregel had large aggregates these were broken up using bath sonicator. The pH of solution was adjusted to 5.3 using 0.1 N NaOH solution, and was stirred for further 30 min. All samples were centrifuged at 1100 rpm for 15 min to remove any large aggregates prior to analysis. Centrifugation under these conditions allowed aggregates to form pellet, leaving nanoparticles suspended in the supernatant. The particle suspension was then centrifuged at 25 °C in the Amicon® Ultra-15 (Ultracel-100K) centrifuge tube with 100 kDa cut off at 5000 rpm for 20 min to separate free polymers from nanoparticles. Nanoparticles in the dialysis tube were evaluated for their size and zeta potential. The solution collected in the outer tube was analyzed spectrophotometrically for loading efficacy.

2.3. Particle characterization

Nanoparticles size and zeta potential were assessed by photon correlation spectroscopy (PCS) using a Malvern zeta sizer ZS series and Scattering Particle Size Analyzer (Malvern Co., UK). For this, a sample of 2 ml was sonicated for 2 min in the bath sonicator, placed in the analyzer chamber and measured immediately.

Nanoparticles morphology such as shape and occurrence of aggregation phenomena was studied by SEM. For this, samples of nanoparticles were mounted on metal stubs, plating coated under vacuum and then examined on a LEO*1455 VP* (10 kV Cambridge) scanning electron microscopy.

2.4. Loading efficacy

For quantitative determination of ODNs loading, samples were centrifuged in an Amicon® Ultra-15 (Ultracel-100K Millipore Co., USA) with a molecular weight cut off of 100 kDa to remove free molecules of polymer and ODNs as well, which are not loaded in the particles. The placebo particles were prepared separately to use as blank solution in subsequent spectrophotometrical analysis. Samples were centrifuged in Amicon® Ultra-15 (Ultracel-100K) for 20 min at 5000 rpm, and then the absorbance of the solutions in the tubes was measured at 260 nm using a UV/VIS spectrophotometer (Jasco V-530, Jasco Co., Japan). The amount of ODN associated with the nanoparticles was calculated by the difference between the initial amount of ODN added to the Chitosan and the amount measured in the supernatant. The following equation was used to determine the loading efficacy of the nanoparticles:

Table 1
Variables used in Box–Behnken experimental design.

Independent variables	Symbol	Levels		
		−1	0	1
Polymer	A	0.5	0.75	1.0
$CaCl_2$	B	0.1	0.2	0.3
N/P	C	5	15	25

Dependent variables	Units	Constraints
Y_1 = particle size	nm	Minimize
Y_2 = loading	%	Maximize

$$\text{Loading efficacy } (LE\%) = \frac{\text{ODN}_{\text{total}} - \text{ODN}_{\text{supernant}}}{\text{ODN}_{\text{total}}} \times 100 \quad (1)$$

Douglas and Tabrizian (2005).

2.5. FTIR analysis

FTIR spectra were obtained using 8400S (Shimadzu Co., Japan) FTIR- spectrometer. Samples were dried in a vacuum desiccator, mixed with micronised KBr powder and compressed into discs using a manual tablet press.

2.6. DSC analysis

DSC thermograms were obtained using (Shimadzu Co., Japan) DSC-60 system. Samples were dried in a vacuum desiccator, 2.0 mg of the dried powder crimped in a standard aluminum pan and heated from 20 to 350 °C at a heating rate of 10 °C/min under constant purging of nitrogen.

2.7. Experimental design

Response surface methodology (RSM) as a statistical and mathematical method fit the experimental data to the model for optimization processes (Myers & Montgomery, 2002). A response surface method, Box–Behnken experimental design (Box & Behnken, 1960) can be used to evaluate the relationship between the independent variables and their responses as well as their interactions in an effective model. In addition, this kind of experimental design can detect the curvature in the response, appropriately. Box–Behnken design needs only three levels in comparison to five levels of central composite design. Therefore, less experiment needs to be carried out.

Independent variables, including (Alg/Chi) ratio (A), $CaCl_2$/Alg (%) (B) and N/P ratio (C) were defined in three levels (low, basal and high) coded: (−,0,+). According to the Box–Behnken design generated by Design-Expert (Version 7.0.0, Stat-Ease, Inc., Minneapolis, MN, USA), 17 experiments including 12 factorial points with five replicates at the center point for estimation of pure error sum of squares were employed. The codes, ranges of levels of the independent variables and the design matrix in coded were shown in Tables 1 and 2, respectively. In Table 2, the values (Y_1) and (Y_2) for each run are the average of three responses.

Table 2
Box–Behnken experimental design in various runs and the correspondent response.

Run no.	Independent variables			Dependent variables	
	A	B	C	Y_1 Particle size (nm)	Y_2 Loading efficacy (%)
1	0	0	0	906	46.7
2	0	−1	1	1090	44.5
3	1	0	−1	888	37.3
4	1	1	0	721	70.3
5	−1	1	0	315	97.8
6	−1	0	1	194	95.6
7	1	0	1	430	66.5
8	0	−1	−1	749	97.8
9	0	0	0	448	100.0
10	0	1	−1	414	98.9
11	0	0	0	1435	75.8
12	−1	0	−1	439	100.0
13	1	−1	0	800	85.2
14	0	0	0	548	85.7
15	0	0	0	777	83.0
16	−1	−1	0	954	81.3
17	0	1	1	750	83.5

The mathematical relationship of the responses (Y_1, Y_2) (particle size and loading efficacy) and the independent variables (X_i) were modeled by a second-order polynomial function as follows:

$$Y = \beta_0 + \beta_1 X_1 + \beta_2 X_2 + \beta_3 X_3 + \beta_{11} X_1^2 + \beta_{22} X_2^2 + \beta_{33} X_3^2 + \beta_{12} X_1 X_2 + \beta_{13} X_1 X_3 + \beta_{23} X_2 X_3 \quad (2)$$

where Y is the predicted response, β_0, intercept, β_1, β_2 and β_3, linear coefficients, β_{11}, β_{22} and β_{33}, squared coefficients and β_{12}, β_{13} and β_{23}, the interaction coefficients of the equation and X_1, X_2 and X_3 are the independent variables. Using this equation, it is possible to evaluate the linear, quadratic and interactive effects of the independent variables on the responses appropriately.

The statistical analysis of the data through regression model and plotting the response surface graphs were achieved by Design-Expert. ANOVA through Fisher's test evaluated the significant effect of the independent variables on the responses and fitted by *p-value <0.05.* The quality indicators for the fitness of the second-order polynomial model equation evaluated by multiple correlation coefficients (R^2) and adjusted R^2. In order to show the relationship and interaction between the coded variables and the response graphically, the three-dimensional surface plot or contour plots were employed in this study. Both numerical and grid searches in whole experimental regions were employed to find the optimized formulations by considering the constraints in which the particle size is in its minimum and loading efficacy (%) in maximum levels. Consequently, five optimized checkpoint formulations were prepared and the experimental responses were compared by the predicted values obtained by the equation to evaluate the precision of the model.

3. Results and discussion

3.1. Nanoparticle size

Nanoparticles ranging from 194 to 1435 nm were obtained through different 17 designed experiments in this study (Table 2). SEM of spherical nanoparticles is shown in Fig. 1.

Nanoparticles were prepared by three different ratios of Alg/Chi, Calcium Chloride/Alginate ($CaCl_2$/Alg) and N/P whilst pH was set at 5.3 in all the experiments as Chitosan is intrinsically poorly water soluble at neutral or alkaline pH, so its solution was prepared in acidic pH. Chitosan is likely to precipitate out from solution upon addition of an Alginate in higher pH, resulting in less Chitosan available for nanoparticles formation. While the pK_a of Chitosan is known to be 6.5 (Chellat et al., 2000), an Alginate solution of neutral pH, upon addition, would result in the majority of amine groups of Chitosan being unprotonated and, therefore, unable to participate in ionic interactions with Alginate. A few protonated groups available for interaction would result in weaker electrostatic interactions with the Alginate gel, leading to larger particle sizes to be produced. Using an Alginate solution with a slightly lower pH 5.3 resolves these problems by allowing a stronger interaction between Chitosan and Alginate, leading to the formation of more compact nanoparticles (Douglas & Tabrizian, 2005). Some other researchers investigating Chitosan for the preparation of nanoparticles, microparticles and polyionic systems have reported working around the same pH (5.0–6.3) (Barichello et al., 1999; Chellat et al., 2000; Douglas & Tabrizian, 2005).Within this range the carboxyl group of the Alginate is ionized and the amine group of the Chitosan is protonated, which is most important for optimum interaction and the polyionic complex formation. Similar observations have been reported in the formation of other polyionic complexes containing Chitosan (Sarmento, Ferreira, Veiga, & Ribeiro, 2006).

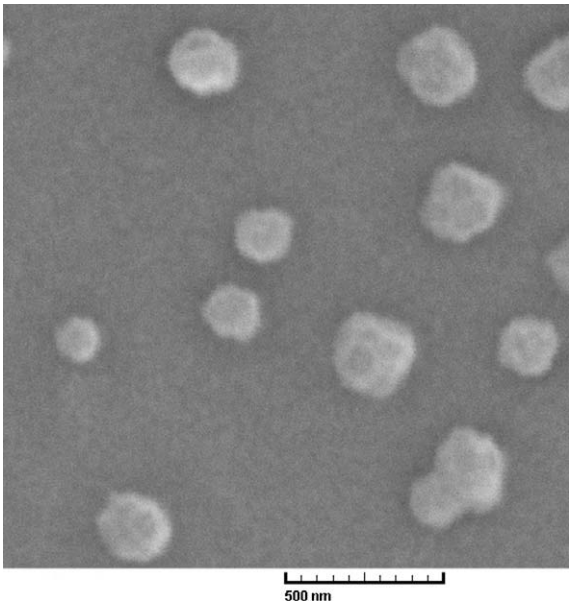

Fig. 1. SEM micrographs of Alginate/Chitosan nanoparticles produced with Alg/Chi ratio of 1, $CaCl_2$/Alg ratio of 0.2% and N/P ratio of 5 at pH 5.3.

3.2. Determination of zeta potential

The stability of many colloidal systems is directly related to the magnitude of their zeta potential. In general, if the value of the particle zeta potential is large, the colloidal system will be stable. Conversely, if the particle zeta potential is relatively small, the colloidal system will agglomerate. The surface charge of the particles is of substantial importance in all the production steps of these particles because the efficiency of the different steps is directly related to the establishment of electrostatic interactions.

Zeta potential of all the nanoparticles prepared was measured by Malvern zeta sizer ZS (data not shown). Nanoparticles which were prepared by Alg/Chi ratio 1:1 showed zeta potential of about +30 mV. This relatively high positive value was due to cationic nature of Chitosan and Alg/Chi ratio (De and Robinson, 2003; Douglas & Tabrizian, 2005).

Thus it has been suggested that the nanoparticles which were prepared in optimum condition and mentioned above may be a good candidate for the delivery of oligonucleotide molecules because of their positive zeta potential leading them to bind with these molecules.

3.3. Box–Behnken design and response surface methodology

The Response surface methodology followed by Box–Behnken design was applied to find optimal level of independent variables including Alg/Chi ratio, Ca/Alg (%) and N/P ratio shown in Table 2. The Design-Expert was used to design the matrix and statistical analysis. Table 1 represents factors in coded forms, the particle size and loading efficacy as the response. According to the data obtained by this design, the range of particle size was found in the range of 194–1435 (nm) and the loading efficacy was 37–100%, respectively. To choose the best model matched with the data, the analysis of variance by calculating *F*-value was employed. As a result, for both responses a full quadratic second-order polynomial equation was fitted to the data appropriately. The lack of fit *F*-value of 0.4673 and 0.4436 implied that the lack of fit was not significant in both responses, due to the pure error and showed adequacy of the models (Tables 3 and 4). The multiple regression analysis by the software showed that all the linear, squared and interaction coefficients of the independent factors including Ca/Alg (%) and N/P ratio were significant ($p < 0.05$) when particle size is considered as the response (Table 3). Therefore, the equation fitted to the data was presented as follows:

$$Y_1 = 739.16 - 177.13X_2 + 210.25X_3 - 240.50X_2X_3 + 195.39X_2^2 - 283.86X_3^2 \quad (3)$$

where Y_1 is the particle size, X_2 and X_3 are $CaCl_2$/Alg and N/P ratio, respectively. As Table 3 shows, the coefficient of determination (R^2) and adjusted R^2 of this model were 0.84 and 0.76, respectively. This means that, 84% variability in the response will be explained by this model. When loading efficacy was considered as the response the results were much better. R^2 and adjusted R^2 of this model were 0.996 and 0.992, respectively (Table 4). Therefore, the similarity between R^2 and adjusted R^2 shows the adequacy of the model to predict the response by optimization process. The predicted R^2 with the value of 0.972 showed very good agreement between the predicted value using the model and the experimental data. In addition, the coefficient value of variation (CV% = 2.27) which was an estimate of the standard deviation associated with experiment around the mean, showed more precision and reliability of the model. The plot of studentized residual versus the values predicted by the model showed no trend which indicating the homogeneity of variance in the data and absence of outliers in the experimental data (not shown). Hence, it can be concluded that the following full quadratic second-order polynomial equation was adequate to model the loading efficacy over the independent variable ranges in this study:

Table 3
The analysis of variance table for particle size as the response (Y_1).

Source	Sum of squares	df	Mean square	*F*-Value	*p*-Value[a] Prob > *F*
Model	1312840.518	5	262568.1036	11.25436	0.0005
B-$CaCl_2$	250986.125	1	250986.125	10.75793	0.0073
C-N/P	353640.5	1	353640.5	15.15797	0.0025
BC	231361	1	231361	9.916744	0.0093
B^2	161200.6579	1	161200.6579	6.909487	0.0235
C^2	340200.5329	1	340200.5329	14.58189	0.0028
Residual	256633.7171	11	23330.33792		
Lack of fit	172232.9171	7	24604.70244	1.166089	0.4673
Pure error	84400.8	4	21100.2		
Cor. total	1569474.235	16			
R^2	0.84				
Adj. R^2	0.76				

[a] Significant at 0.05 level.

Table 4
The analysis of variance table for loading efficacy as the response (Y_2).

Source	Sum of squares	df	Mean square	*F*-Value	*p*-Value[a] Prob > *F*
Model	6581.427551	9	731.2697279	224.2802	<0.0001
A-polymer	449.2503125	1	449.2503125	137.785	<0.0001
B-$CaCl_2$	196.02	1	196.02	60.11928	<0.0001
C-N/P	341.2578125	1	341.2578125	104.6637	<0.0001
AB	309.76	1	309.76	95.00331	<0.0001
AC	281.400625	1	281.400625	86.3055	<0.0001
BC	160.0225	1	160.0225	49.07886	<0.0002
A^2	1544.699533	1	1544.699533	473.759	<0.0001
B^2	933.681375	1	933.681375	286.3598	<0.0001
C^2	2599.310059	1	2599.310059	797.2077	<0.0001
Residual	22.823625	7	3.260517857		
Lack of fit	10.360625	3	3.453541667	1.108414	0.4436
Pure error	12.463	4	3.11575		
Cor. total	6604.251176	16			
R^2	0.996				
Adj. R^2	0.992				
Predicted R^2	0.972				

[a] Significant at 0.05 level.

$$Y_2 = 83.72 + 7.49X_1 + 4.95X_2 - 6.53X_3 + 8.80X_1X_2 + 8.39X_1X_3 + 6.32X_2X_3 - 19.15X_1^2 - 14.89X_2^2 + 24.85X_3^2 \quad (4)$$

where Y_2 is loading efficacy, X_1 is the polymer ratio, X_2 is the $CaCl_2$/Alginate (%) and X_3 is the N/P ratio.

The 3D response surfaces plotted by Design-Expert software of the independent variables on both responses (Y_1 and Y_2) are shown in Figs. 2 and 3a–c. In each plot, the interaction of two variables was investigated simultaneously while the third one was in its middle level value. As a result, in Fig. 2a, the response surface showed a curvature along the $CaCl_2$ axis which indicates the statistical significance of quadratic coefficients of $CaCl_2$/Alg in the model, while the polymer ratio seems to have no significant effect on the particle size. The reduction of particle size with increasing $CaCl_2$ amount reacted with Alginate, from 0.1% to 0.2% was in line with the initial hypothesis and can be explained by what is known about the interaction between Alginate and divalent cations. These cations bind preferentially with guluronic acid blocks of the Alginate macromolecule due to their "Zig-Zag" structure that can more readily accommodate those (Cafaggi et al., 2007). De and Robinson (2003) reported that insufficient interaction occurred below a mass ratio of ($CaCl_2$/Alg 0.2%) to cause detectable gelation or microparticle formation occurred. In their study the mass ratio region of 0.2–0.6%, there was a sigmoidal increase in turbidity this is the region where maximum aggregation and gelation occurs due to cooperative binding between Calcium ions and the Guluronic and Mannuronic acid residues. While this weight ratio region is necessary to prepare microspheres, it prevented the formation of nanospheres. It has been postulated that the pregel state was necessary to enable the ionic interactions between Alginate and Chitosan to form nanosphere. Formation of nanospheres required a low concentration of $CaCl_2$ (less than 0.2% mass ratio) to form the negatively charged, Calcium Alginate pregel that was subsequently enveloped by the positively charged Chitosan. Cationic polymers restrict further cooperative binding between Calcium and Alginate ions.

As shown in Fig. 2b, the minimum levels of particle size were measured near low levels of both Alg/Chi and N/P ratio. Increasing N/P ratio from 5 to 25 led to an increase in particle size from 315 to749 nm. The zeta potential of nanoparticles at N/P ratio of 5 was 25 mV. It was also reported that the zeta potential of nanoparticles increases in an N/P ratio-dependent manner. Briefly, all the nanoparticles appeared to have a positive surface charge and the zeta potential value above an N/P ratio of 5 was saturated. They reported that at N/P ratio of 5, ODN molecules were completely condensed (Kim & Kim, 2007). Saturation of nanoparticles with positive surface charge may be the cause of increasing size of nanoparticles with increasing N/P ratios. Kim and Kim also reported that in the case of water soluble Chitosan-based nanoparticles loaded with IL-5 AS-ODN, particle size increased with increasing N/P ratio from 1 to 10.

The effect of Alg/Chi ratio and interaction effect of Alg/Chi and N/P ratios was not statistically significant ($p > 0.05$) (Fig. 2a). For the preparation of nanoparticles, polymers weight ratios were selected according that reported by Douglas and co-workers (2005) to ensure that all batches of Alg/Chi nanospheres had submicron size with the smallest possible size (Alg/Chi ratios of 1, 0.75 and 0.5). Within this range the functional groups of the polymers were coincided to their stoichiometric proportion. It was also reported that molecular weight of polymers had a great influence on particle size and that the 1:1 polymer ratio at pH 5.3 could result in the smallest nanoparticle size. Furthermore, the 1:1.5 and 1.5:1 ratios also resulted in small size compared to the other ratios they used, but in this study there was no significant difference between the ratios of 1, 0.75 and 0.5.

In Fig. 2c the curvature in both variables was quite obvious while, the direction of these curvatures was different. This could be predicted from the sign of X_2^2 and X_3^2 in Eq. (1). The convex shape of the plot shown in Fig. 3a indicates that we could find the optimum value (maximum value) for the response in the range of variables studied. The loading efficacy increased when both Alg/Chi ratio and CaCl2/Alg % increase to reach a maximum and then decreased at the combination of the high level of variables. This observation may be caused by decreasing capacity of nanoparticles to encapsulate ODNs. Reducing the Alg/Chi ratio could cause decreasing electrostatic attraction and increasing Alg/Chi ratio could lead to aggregation, so the optimum ratio needs to be found to obtain the highest loading efficacy.

Motwani et al. (2008) also reported that Chitosan concentration had a negative effect on the loading efficacy, because at higher concentrations Chitosan led to the formation of aggregates upon addition of Alginate.

Fig. 3b shows that N/P ratio also affected the loading efficacy; it means that loading efficacy could be decreased from 97.8 to 66.45 (%) with increasing the N/P ratio from 5 to 25. This may be due to increasing particle size with increasing N/P ratio which was discussed above. With particle size reduction, the effective surface area increases, resulting in ODNs binding more efficiently to the particles and leading to improvement in the loading efficacy.

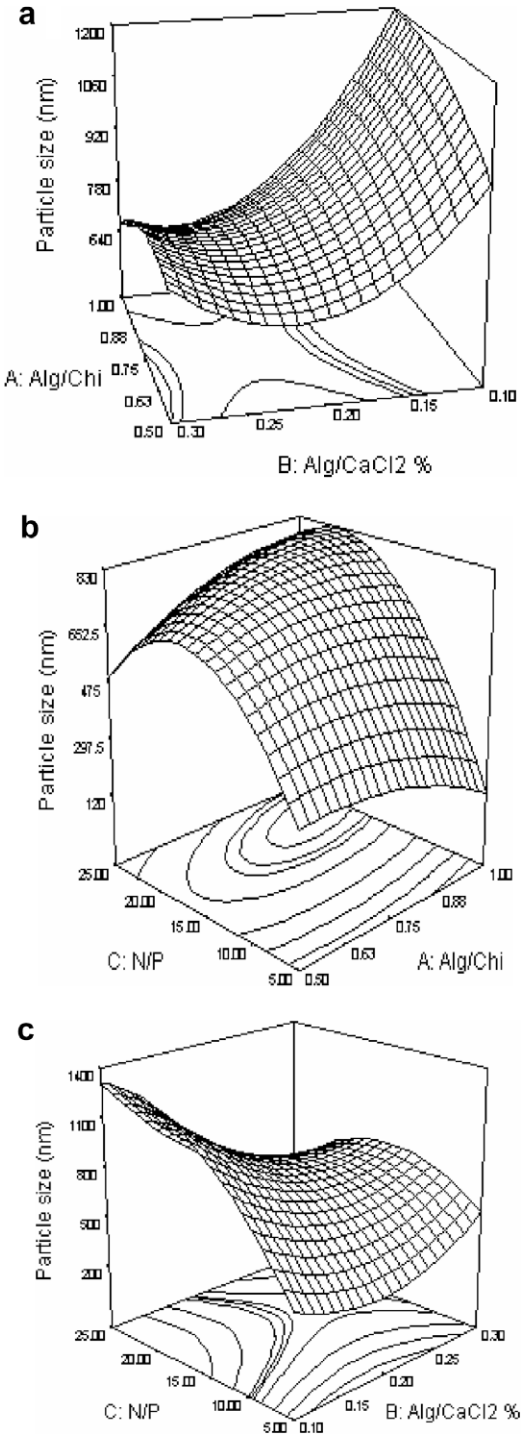

Fig. 2. 3D response surface plots for particle size analysis.

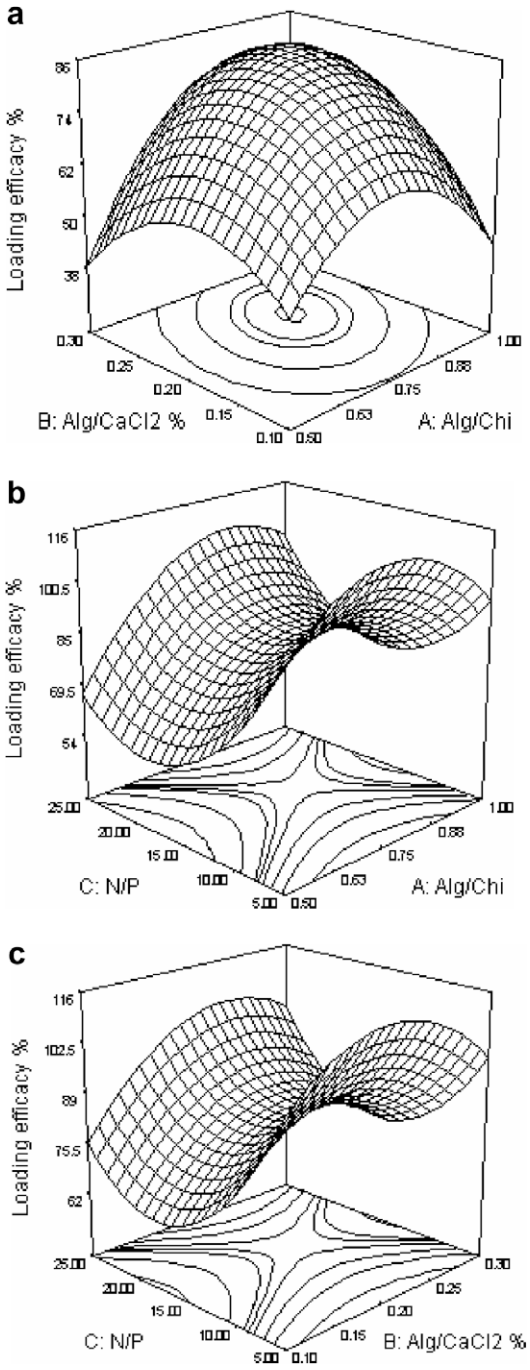

Fig. 3. 3D response surface plots for loading efficacy analysis.

3.4. Optimization

By analysis of response surface plots obtaining by Design-Expert software and numerical solution for Eqs. (3), (4) and constraints, the optimum values for independent variables in uncoded (actual) units to minimize the particle size and maximize the loading responses were Alg/Chi ratio 1, $CaCl_2$/Alg (%) 0.2 and N/P ratio 5, respectively. According to these conditions, the particle size and loading efficacy predicted by the model calculated as 194 nm and 95.6%, respectively. For validation of the model, five experiments were performed by using the optimum condition as mentioned previously. The perfect agreement between the observed values and the values predicted by the equation confirms the statistically significance of two models as well as their adequate precision for the prediction of optimum conditions in the domain of levels chosen for the independent variables.

3.5. FTIR evaluation

In order to examine the interaction between components of nanoparticulate systems, preliminary concerns were taken over polyelectrolytes interactions. It is well established that the carboxyl group of the anionic polymer may interact with the amino group of Chitosan and form an ionic complex (Riberio et al.,

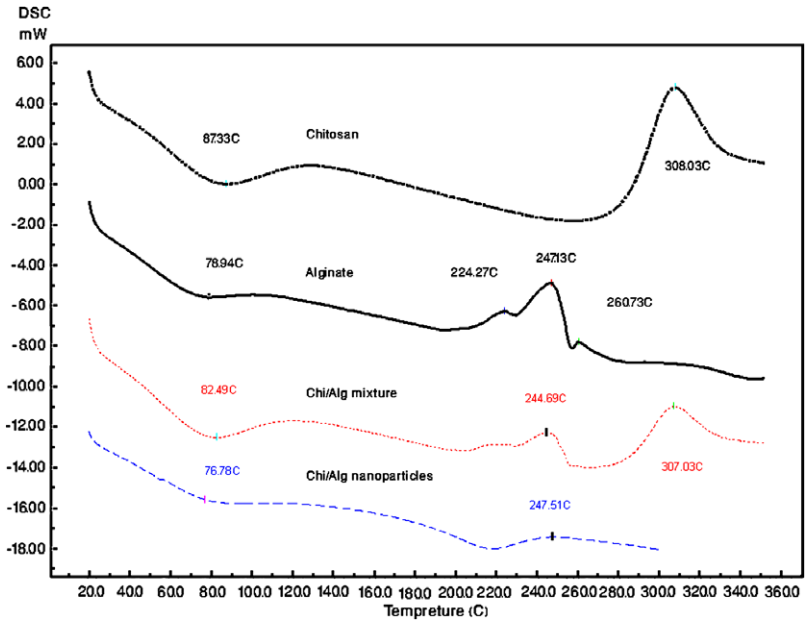

Fig. 4. Thermograms of Alginate, Chitosan, Alginate/Chitosan mixture and nanoparticles produced with 1:1 Alg/Chi ratio, 0.2% Ca/Alg ratio, 0.2% Ca/Alg ratio.

2005). As a result, there were changes in the absorption bands of amino groups, carboxylic groups, and amide bonds in FTIR spectra. Consequently, after complexation with Chitosan Alginate carboxyl peaks near 1631, and 1425 cm^{-1} broaden and shift slightly from 1650 to 1610 cm^{-1} and 1411 cm^{-1}, respectively. The FTIR spectrum of Chitosan also showed a peak of amide bond at 1650 cm^{-1} and a strong protonated amino peak at 1596 cm^{-1} because it is obtained from partial N-deacetylation of chitin. However, both peaks were shifted after complexation with Alginate, the amide peak into singlet bond at 1610 cm^{-1} and the amino peak to 1534 cm^{-1} (figure not shown). Observed changes in the absorption bands of the amino groups, carboxyl groups, and amide bonds could be attributed to an ionic interaction between the carbonyl group of Alginate and the amide group of Chitosan (Sarmento et al., 2006).

3.6. DSC evaluation

DSC thermogram of Chitosan showed an initial endothermic peak at 82.49 °C and a higher exothermic peak at 308.03 °C (Fig. 4). Alginate showed an initial endothermic peak at 78.94 °C and exothermic peak at 224.27, 247.13, and 260.73 °C. Endothermic peaks were correlated with loss of water associated to hydrophilic groups of polymers while exothermic peaks result from degradation of polyelectrolytes due to dehydration and depolymerisation reactions most probably to the partial decarboxylation of the protonated carboxylic groups and oxidation reactions of the polyelectrolytes.

Thermogram of Alginate/Chitosan physical mixture showed a broader endothermic peak at 82.49 °C, which probably represents the combination of the two endothermic polymer peaks. Exothermic peaks at 220.2, 244.69, and 307.03 °C resulted from individual contribution of Alginate and Chitosan, respectively. It could be seen that the peaks of the complexes were shifted from those of physical mixture. Peaks of physical mixture appeared to be combination of each material but they were different from those of nanoparticles probably because complexation of polyelectrolytes resulted in new chemical bonds. Exothermic peak of Alginate/Chitosan nanoparticles was recorded at 247.5 °C, an intermediate and broader peak value compared with individual polyelectrolytes, which was interpreted as an interaction between both components (Riberio, Silva, Ferreira, & Vega, 2005; Sarmento et al., 2006).

4. Conclusion

Preparation and optimization of Alg/Chi nanoparticles were the goals of this study. Some parameters like Alg/Chi ratio, $CaCl_2$/Alginate (%) ratio and N/P ratio that can affect the size and loading efficacy of these particles were identified. the optimum conditions for preparation of Alginate–Chitosan nanoparticles was Alg/Chi ratio of 1, $CaCl_2$/Alg ratio of 0.2% and N/P ratio of 5 at pH 5.3. DSC can successfully be used to characterize the nanoparticles made up by polyelectrolyte complexes and in our study it was shown that an interaction takes place between polyelectrolytes to make nanoparticles. Because of the positive zeta potential of the smallest nanoparticles which were made as part of this study and their good loading efficacy 95.6 (%), these nanoparticles are promising for their application in gene delivery which is the main goal of our future study.

Acknowledgement

The authors wish to thank the vice-chancellor in research affairs of Tehran University of Medidical sciences for financial support of this investigation.

References

Arteaga, C. L. (2002). Epidermal growth factor receptor dependence in human tumors: More than just expression? *Oncologist, 7*, 31–39.

Barichello, J. M., Morishita, M., Takayama, K., & Nagai, T. (1999). Encapsulation of hydrophilic and lipophilic drugs in PLGA nanoparticles by the nano-precipitation method. *Drug Development and Industrial Pharmacy, 25*, 471.

Borchard, G. (2001). Chitosans for gene delivery. *Advanced Drug Delivery Reviews, 52*, 145.

Box, G. E. P., & Behnken, D. W. (1960). Some new three level designs for the study of quantitative variables. *Technometrics, 2*, 455–475.

Cafaggi, S., Russo, E., Stefani, R., Leardi, R., Caviolglioli, G., Parodi, B., et al. (2007). Preparation and evaluation of nanoparticles made of chitosan or N-trimethyl chitosan and a cisplatin–alginate complex. *Journal of Controlled Release, 121*, 110–123.

Chellat, F., Tabrizian, M., Dumitriu, S., Chornet, E., Magny, P., Rivard, C. H., et al. (2000). *In vitro* and *in vivo* biocompatibility of chitosan–xanthan polyionic complex. *Journal of Biomedical Materials Research, 51*, 107–113.

De, S., & Robinson, D. (2003). Polymer relationships during preparation of chitosan–alginate and poly-L-lysine–alginate nanospheres. *Journal of Controlled Release, 89*, 101.

Douglas, K. L., & Tabrizian, M. (2005). Effect of experimental parameters on the formation of alginate–chitosan nanoparticles and evaluation of their potential application as DNA carrier. *Journal of Biomaterials Science. Polymer Edition, 1*, 43–56.

Fundueanu, G., Nastruzzi, C., Carpov, A., Desbrieres, J., & Rinaudo, M. (1999). Physico-chemical characterization of Ca-alginate microparticles produced with different methods. *Biomaterials, 20*, 1427.

Kim, S. T., & Kim, C. K. (2007). Water-soluble chitosan-based antisense oligodeoxynucleotide of interleukin-5 for treatment of allergic rhinitis. *Biomaterials, 28*, 3360–3368.

Madan, T., Munshi, N., De, T. K., Maitra, A., Sarma, P. U., & Aggarwal, S. S. (1997). Biodegradable nanoparticles as a sustained release system for the antigens/allergens of *Aspergillus fumigatus*: Preparation and characterisation. *International Journal of Pharmaceutics, 159*, 135.

Mansouri, S., Lavigne, P., Corsi, K., Benderdour, M., Beaumont, E., & Fernandes, J. C. (2004). Chitosan–DNA nanoparticles as non-viral vectors in gene therapy: Strategies to improve transfection efficacy. *European Journal of Pharmaceutics and Biopharmaceutics, 57*, 12.

Mi, F.-L., Sung, W., & Shyu, S.-S. (2002). Drug release from chitosan–alginate complex beads reinforced by a naturally occurring cross-linking agent. *Carbohydrate Polymers, 48*, 61.

Motwani, S. K., Chopra, Sh., Talegaonkar, S., Kohli, K., Ahmad, F. J., & Khar, R. K. (2008). Chitosan–sodium alginate nanoparticles as submicroscopic reservoirs for ocular delivery: Formulation, optimisation and in vitro characterization. *European Journal of Pharmaceutics and Biopharmaceutics, 68*, 513–525.

Myers, R. H., & Montgomery, D. (2002). *Response surface methodology: Process and product optimization using designed experiments* (2nd ed.). New York: Wiley.

Riberio, A. J., Silva, C., Ferreira, D., & Vega, F. (2005). Chitosan-reinforced alginate microspheres obtained through the emulsification/internal gelation technique. *European Journal of Pharmaceutical Sciences, 25*, 31–40.

Sarmento, B., Ferreira, D., Veiga, F., & Ribeiro, A. (2006). Characterization of insulin-loaded alginate nanoparticles produced by ionotropic pre-gelation through DSC and FTIR studies. *Carbohydrate Polymers, 66*, 1–7.

Yan, X. L., Khor, E., & Lim, L. Y. (2001). Chitosan–alginate films prepared with chitosans of different molecular weights. *Journal of Biomedical Materials Research, 58*, 358.